essentially just enantiomorphs. A complete table of torsion angles is available as supplementary material, but in Table VI we present mean values of the most pertinent ones for the principal and minor molecules. It can be seen that differences are small. In addition, the validity of our description of these rings as half-chairs is shown by the fact that, in each case, the Re atoms lie above and below the mean P—C=C—P planes by approximately equal amounts as would be expected from the drawing in Figure 4.

It is worth mentioning that the next best conformation for cyclohexene itself is a half-boat (ca. 3 kcal mol^{-1} less stable). The analogue to that in the present case is illustrated schematically in III, where it can be seen that because of the large phenyl substituents it is understandably disfavored here.

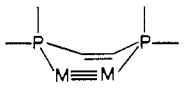

III

In conclusion, then, the introduction of the "stiffened backbone" in dppee, as contrasted with the flexible backbone in dppe, leads to certain changes in the conformational characteristics of these molecules. These conformational changes then have consequences with respect to the way in which the molecules are assembled in the complete crystal structure.

Acknowledgment. Support from the National Science Foundation (Grant No. CHE85-14588 to F.A.C. and Grant No. 85-06702 to R.A.W.) is gratefully acknowledged.

Registry No. α-$Re_2Cl_4(dppee)_2$·*n*-PrOH, 114720-22-8; β-$Re_2Cl_4(dppee)_2$, 110329-68-5; α-$Re_2Cl_4(dppe)_2$, 114720-23-9; $(n\text{-}Bu_4N)_2Re_2Cl_8$, 14023-10-0; $[ReCl_2(dppe)_2]Cl$, 15628-22-5; $(n\text{-}Bu_4N)_2Re_2Br_8$, 14049-60-6; α-$Re_2Br_4(dppe)_2$, 114720-24-0; α-$[Re_2Cl_4(dppee)_2]PF_6$, 114720-26-2; $(Cp_2Fe)PF_6$, 11077-24-0; α-$[Re_2Cl_4(dppp)_2]PF_6$, 114720-28-4; α-$Re_2Cl_4(dppp)_2$, 86436-61-5; Re, 7440-15-5; α-$Re_2Cl_4(dppee)_2$, 110329-67-4.

Supplementary Material Available: Full tables of bond distances and bond angles and tables of anisotropic displacement parameters for α-$Re_2Cl_4(dppee)_2$·*n*-PrOH and β-$Re_2Cl_4(dppee)_2$ and a table of torsional angles for the β isomer (14 pages); listings of observed and calculated structure factors for both compounds (45 pages). Ordering information is given on any current masthead page.

Contribution from the Anorganisch Chemisch Laboratorium, J. H. van 't Hoff Instituut, University of Amsterdam, 1018 WV Amsterdam, The Netherlands, Department of Inorganic Chemistry, University of Nijmegen, Toernooiveld, 6525 ED Nijmegen, The Netherlands, and Department of Chemistry, University of Edinburgh, Edinburgh EH9 3JJ, Scotland, U.K.

Syntheses and Characterization of Unique Organometallic Nickel(III) Aryl Species. ESR and Electrochemical Studies and the X-ray Molecular Study of Square-Pyramidal $[Ni\{C_6H_3(CH_2NMe_2)_2\text{-}o,o'\}I_2]$

David M. Grove,[1a] Gerard van Koten,*[,1a] Pim Mul,[1a] Rob Zoet,[1a] Johannes G. M. van der Linden,[1b] Johan Legters,[1b] John E. J. Schmitz,[1b] Nicholas W. Murrall,[1c] and Alan J. Welch[1c]

Received August 6, 1987

Oxidation of the Ni(II) species [Ni(*NCN'*)X] (*NCN'* = $C_6H_3(CH_2NMe_2)_2$-*o*,*o'*) by appropriate reagents [CuX_2 (X = Br, Cl), I_2 (X = I)] affords in high yield the unique five-coordinate Ni(III) aryl species [Ni(*NCN'*)X_2] (X: Br, **1a**; Cl, **1b**, I, **1c**) that are precursors to the NO_3 and NO_2 analogues **1d** and **1e**, respectively. ESR data for **1a**–**e** indicate a d^7 electronic configuration with a single unpaired electron in the d_{z^2} orbital; a low-spin configuration is also consistent with the magnetic susceptibility of 1.989 (3) μ_B found for **1c**. The iodo analogue **1c** has also been the subject of an X-ray crystallographic study that established a square-pyramidal coordination geometry for the Ni(III) center. Crystals of **1c**, $C_{12}H_{19}NiN_2I_2$, are monoclinic, space group $P2_1/c$, with a = 13.9696 (9) Å, b = 7.8683 (9) Å, c = 15.0510 (17) Å, β = 108.769 (7)°, V = 1566.4 Å^3, Z = 4, d_{calcd} = 2.136 cm^3, $F(000)$ = 956 e, μ(Mo K$\bar{\alpha}$) = 48.6 cm^{-1}. On the basis of 3365 unique reflections with $F_o > 2.0\sigma F_o$, the structure has been refined to R = 0.0499 and R_w = 0.0603. Within the nickel coordination sphere one iodine atom I2, the aryl C1 atom, and the mutually trans N-donor atoms of *NCN'* define the square base, while the second iodine atom I1 is at the pyramid apex; the Ni atom lies ca. 0.325 Å above the plane of the basal atoms. Conductivity measurements on **1b** and **1d** show full dissociation of both X anions in aqueous solution. In acetone solution, where dissociation is not significant, [Ni^{II}(*NCN'*)X] and [Ni^{III}(*NCN'*)X_2] are electrochemically interconvertible when additional X anion is present. The $E_{1/2}$ value for the redox couple [Ni(*NCN'*)$(H_2O)]^+$/[Ni(*NCN'*)$(H_2O)_n]^{2+}$ in H_2O is +0.14 V (vs SCE). The importance of organometallic nickel(III) species is discussed, with particular respect being paid to their intermediacy in oxidative-addition reactions.

Introduction

Recent studies have shown that certain systems of biological interest, principally hydrogenases, may contain paramagnetic centers attributable to the less common Ni(III) state.[2,3] As would be anticipated, hard donor atoms are suitable for stabilizing the higher oxidation states of nickel, and many inorganic Ni(III) species have been reported containing nitrogen-donor macrocyclic ligands.[3]

Our studies on the coordination properties of the monoanionic terdentate ligand $C_6H_3(CH_2NMe_2)_2$-*o*,*o'* (*NCN'*) show that it can form square-planar Ni(II),[4] Pd(II),[5] and Pt(II)[5] complexes. These organometallic species, which contain two trans N-donor sites and a M–C σ-bond, have relatively good thermal stability, and this property has allowed an electronic structure study of certain members by ultraviolet photoelectron spectroscopy.[6] In the present report it is shown that unique air-stable square-pyramidal Ni(III) species [Ni(*NCN'*)X_2] (X: Cl, **1a**; Br, **1b**; I, **1c**) (Figure 1) result from either chemical or electrochemical oxidation of the corresponding Ni(II) halo species [Ni(*NCN'*)X] (**2a**–**c**). Characterization of these species, the first reported true organometallic

(1) (a) University of Amsterdam. (b) University of Nijmegen. (c) University of Edinburgh.
(2) (a) Albracht, S. P. J.; Van der Zwaan, J. W.; Fontijn, R. D. *Biochim. Biophys. Acta* **1984**, *766*, 245–288. (b) Lindahl, P. A.; Kojima, N.; Hausinger, R. P.; Fox, J. A.; Teo, B. K.; Walsh, C. T.; Orme-Johnson, W. H. *J. Am. Chem. Soc.* **1984**, *106*, 3062–3064. (c) Okura, I. *Coord. Chem. Rev.* **1985**, *68*, 53–99. See also: *Bioorganic Chemistry of Nickel*; Lancaster, J. R., Jr., Ed.; VCH: Deerfield Beach, FL, in press; and references cited in these publications.
(3) (a) Nag, K.; Chakravorty, A. *Coord. Chem. Rev.* **1980**, *33*, 87–147. (b) Haines, R. I.; McAuley, A. *Coord. Chem. Rev.* **1981**, *39*, 77–119.
(4) Grove, D. M.; Van Koten, G.; Ubbels, H. C. J.; Zoet, R.; Spek, A. L. *Organometallics* **1984**, *3*, 1003–1009.
(5) Grove, D. M.; Van Koten, G.; Louwen, J. N.; Noltes, J. G.; Spek, A. L.; Ubbels, H. J. C. *J. Am. Chem. Soc.* **1982**, *104*, 6609–6616.
(6) Louwen, J. N.; Grove, D. M.; Ubbels, H. J. C.; Stufkens, D. J.; Oskam, A. *Z. Naturforsch., B: Phys., Phys. Chem., Kosmosphys.* **1983**, *38B*, 1657–1664.

0020-1669/88/1327-2466$01.50/0

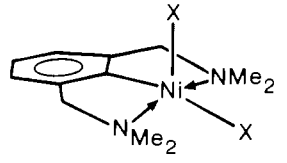

1a X = Cl
1b X = Br
1c X = I
1d X = NO_3
1e X = NO_2

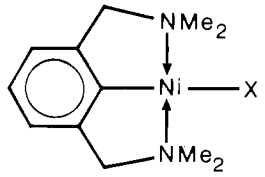

2a X = Cl
2b X = Br
2c X = I
2d X = NO_3
2e X = NO_2

Figure 1. Schematic structures and numbering of [Ni(*NCN*')X_2] and [Ni(*NCN*')X] complexes.

Ni(III) complexes, includes ESR spectroscopy, electrovoltammetry, and an X-ray crystal structure determination of the iodo representative **1c**. The isolation of these complexes has particular relevance to discussions concerning the intermediacy of organonickel(III) species in the oxidative-addition of aryl halides to zerovalent nickel centers. Some aspects of this work have appeared as a communication.[7]

Experimental Section

General Procedures. All reactions were carried out under a N_2 atmosphere with previously dried and distilled solvents unless otherwise stated. All reagents are commercially available except for the complexes [Ni(*NCN*')X] (X = Cl, Br, I) and [Ni(*NCN*')H_2O]$^+X^-$ (X = BF_4), which were synthesized according to published procedures.[4] The syntheses of [Ni(*NCN*')X] and [Ni(*NCN*')X_2] where X is either NO_3 or NO_2 are described elsewhere.[8] Elemental analyses were carried out by the Analytical Section of the Institute for Organic Chemistry TNO, Utrecht, The Netherlands.

Syntheses. [Ni{$C_6H_3(CH_2NMe_2)_2$-*o*,*o*'}X_2] (X: Cl, 1a; Br, 1b). To a stirred suspension of [Ni(*NCN*')X] (X = Cl, Br) (0.5 mmol) in distilled (but not dried) acetone (30 mL) at room temperature was added slightly more than 1 equiv of CuX_2 (0.6 mmol), and an immediate darkening of the solution to either brown-black (X = Cl) or green-black (X = Br) occurred. After 15 min the solution was filtered to remove CuX, and this solid was washed with several 10-mL portions of acetone. The combined filtrate and washings (ca. 120 mL) were evaporated to dryness in vacuo, and the almost-black solid was washed with a little toluene to remove traces of unreacted yellow-orange [Ni(*NCN*')X]. Extraction of the solid with CH_2Cl_2 (30 mL) gave a dark solution that when evaporated to dryness afforded the product in high yield. Slow evaporation of a CH_2Cl_2/toluene (50:50) solution of **1a** or **1b** affords the highly crystalline black products in typically 80–90% yield. Anal. Calcd for $C_{12}H_{19}Cl_2NiN_2$ (**1a**): C, 44.91; H, 5.97; N, 8.72. Found: C, 44.91; H, 5.95; N, 8.76. Calcd for $C_{12}H_{19}Br_2NiN_2$ (**1b**): C, 35.17; H, 4.67; N, 6.84. Found: C, 35.29; H, 4.63; N, 6.68.

[Ni{$C_6H_3(CH_2NMe_2)_2$-*o*,*o*'}I_2] (1c). To a stirred solution of [Ni(*NCN*')I] (200 mg, 0.84 mmol) in benzene (10 mL) was added slightly more than 0.5 equiv of solid I_2 (74 mg, 0.45 mmol). The solution darkened rapidly, and a brown-black precipitate soon formed. After 0.5 h the solvent and volatiles were removed in vacuo, and the dark solid was washed thoroughly with pentane and diethyl ether. Pure product was obtained by dissolution of this solid in CH_2Cl_2, filtration, addition of an equal volume of toluene, and slow evaporation of the solvent using a N_2 stream. Yield: 214 mg (80%) of black crystalline **1c**. Anal. Calcd for $C_{12}H_{19}I_2NiN_2$ (**1c**): C, 28.61; H, 3.80; N, 5.56. Found: C, 28.53; H, 3.77; N, 5.51.

Spectroscopic Measurements. ESR spectra of the complexes in toluene or diglyme glasses were measured on a Bruker ER200D MR X-band spectrometer, and Q-band spectra were measured on a Varian E-9 EPR spectrometer as detailed in ref 2a. Magnetic susceptibility of **1c** was carried out by the Department of Inorganic Chemistry, University of Leiden, under the supervision of Prof. J. Reedijk.

Electrochemical Measurements. These were made with a three-electrode Bruker E310 instrument with platinum working and auxiliary electrodes. Electrochemical studies were made either on acetone solutions with potentials referred to an Ag/AgCl (0.1 mol dm^{-3} LiCl) reference electrode ($E_{1/2}$ ($FeCp_2^+$/$FeCp_2$) = +0.63 V) or on aqueous solutions with potentials referred to the SCE. In both cases the reference electrode was separated from the test solution via a Luggin capillary containing the supporting electrolyte (0.1 M Bu_4NX). Normal- and differential-pulse voltammograms were obtained at a scan rate of 5 mV s^{-1} with a pulse frequency of 2 pulses s^{-1}; the differential-pulse amplitude was 10 mV. Cyclic voltammograms were taken with scan rates of 0.01–20 V s^{-1}. The recording device was a Kipp BD 30 recorder, while cyclic voltammograms with scan speeds greater than 200 mV s^{-1} were displayed on a Tektronix 564B storage oscilloscope or a Nicolet Explorer II Model 206. The potential range employed in water was limited to about −0.5 to +0.8 V (vs SCE) in order to avoid oxide layer formation or hydrogen adsorption on the platinum electrode.[9] In this potential range all the supporting electrolytes used gave sufficiently low currents in blank solutions. Conductivity measurements were made with a Metrohm Konductoskoop E365 and a Philips PR9510 conductance cell.

X-ray Crystallographic Study of [Ni{$C_6H_3(CH_2NMe_2)_2$-*o*,*o*'}I_2] (1c). A single black crystal, ca 0.025 × 0.030 × 0.050 cm, was mounted on a glass fiber with epoxy resin adhesive. Preliminary Weissenberg photography (Cu K$\bar{\alpha}$ X-radiation) yielded the space group and approximate cell dimensions, after which the crystal was transferred to an Enraf-Nonius CAD4 diffractometer. After an initial cell had been generated by the automatic centering of 25 low-angle reflections ($9 < \theta < 13°$, Mo K$\bar{\alpha}$ X-radiation, $\bar{\lambda}$ = 0.71069 Å), an asymmetric fraction of intensity data in the range $17 < \theta < 18°$ was rapidly recorded, from which 25 strong reflections were chosen and centered. The final cell dimensions and orientation matrix were generated by a least-squares fit.

Crystal Data: $C_{12}H_{19}I_2NiN_2$; mol wt 503.8; space group $P2_1/c$ (No. 14); Z = 4; a = 13.9696 (9), b = 7.8683 (9), c = 15.0510 (17) Å; β = 108.769 (7)°; V = 1566.4 Å^3; μ(Mo K$\bar{\alpha}$) = 48.6 cm^{-1}; d_{calcd} = 2.136 cm^{-3}; F(000) = 956; T = 291 ± 1 K.

Collection and Reduction of Data. Three-dimensional intensity data ($+h,+k,\pm l$) were recorded in the range $1.0 < \theta < 28.0°$ with a θ–2θ scan in 96 steps. After a rapid prescan, only those reflections considered sufficiently intense ($I > 1.25\sigma(I)$) were remeasured such that the final net intensity had $I > 50\sigma(I)$ subject to a maximum scan period of 60 s. Two standard reflections were remeasured once every 3600 s of X-ray exposure time, but subsequent analysis of their net count as functions of time showed no crystal decomposition, crystal movement, or source variance over the data collection period of ca. 102 h. Data were corrected for Lorentz and polarization effects and empirically (ψ-scan) for X-ray absorption. Of 3968 symmetry-independent reflections measured, 3365 had $F_o > 2.0\sigma(F_o)$, and these were used for structure solution and refinement.

Solution and Refinement of the Structure. Approximate positions for the nickel and iodine atoms were deduced by analysis of the Patterson function, and subsequent iterative refinement (full-matrix least-squares) and difference electron density syntheses yielded all remaining non-hydrogen atoms. All non-hydrogen atoms were allowed anisotropic thermal vibration. Hydrogen atoms were set in idealized positions (C–H = 1.08 Å) and allowed to ride on their respective carbon atoms with fixed isotropic thermal parameters[10] (U_H = 0.06 Å^2). Structure factors were weighted according to $w^{-1} = [\sigma^2(F_o) + 0.0076(F_o^2)]$, giving no unusual or systematic variation of the root-mean-square deviation of a reflection of unit weight vs parity group, $(\sin\theta)/\lambda$, F_o, h, k, or l. The 166 variable parameters (including an overall scale factor) were optimized by full-matrix least squares (data:variable ratio better than 20:1) that converged at[11] R = 0.0499 and R_w = 0.0603. The maximum residue on the final ΔF synthesis was 1.02 e Å^{-3}.

Structure solution and refinement were carried out by using the SHELX76 system[12] implemented on the Edinburgh Regional Computer Centre ICL 2972 machine. Molecular geometry calculations were made with XANADU[13] and XRAY76[14] and figures constructed by using ORTEP-II.[15]

The final values of the positional parameters of the refined atoms are given in Table I. Anisotropic thermal parameters (Table II) and a

(7) Grove, D. M.; Van Koten, G.; Zoet, R.; Murrall, N. W.; Welch, A. J. *J. Am. Chem. Soc.* **1983**, *105*, 1379–1380.
(8) Grove, D. M.; Van Koten, G.; Mul, W. P.; Van der Zeijden, A. A. H.; Terheijden, J.; Zoutberg, M. C.; Stam, C. H. *Organometallics* **1986**, *5*, 322–326.
(9) Adam, R. N. *Electrochemistry at Solid Electrodes*; Dekker: New York, 1969.
(10) The isotropic temperature factor is defined as $\exp[-8\pi^2U(\sin^2\theta/\lambda^2]$.
(11) $R = \sum||F_o| - |F_c||/\sum|F_o|$; $R_w = [\sum_w||F_o| - |F_c||^2/\sum_w|F_o|^2]$.
(12) Sheldrick, G. M. "SHELX76, A Program for Crystal Structure Determination", University of Cambridge, England, 1976.
(13) Roberts, P.; Sheldrick, G. M. "XANADU, A Program for Crystallographic Calculations", University of Cambridge England, 1976.
(14) Stewart, J. M.; Machin, P. A.; Dickinson, C.; Ammon, H. L.; Heck, H. "The XRAY76 System"; Technical Report TR 446; Computer Science Center, University of Maryland: College Park, MD, 1976.
(15) Johnson, C. K. "ORTEP-II"; Report-ORNL-5138; Oak Ridge National Laboratory: Oak Ridge, TN.

Table I. Fractional Coordinates with Estimated Standard Deviations in Parentheses for [Ni{$C_6H_3(CH_2NMe_2)_2$-*o*,*o*'}I_2] (**1c**)

	x	*y*	*z*
Ni1	0.27814 (4)	0.06844 (7)	0.24667 (4)
I1	0.12635 (3)	0.24123 (5)	0.26611 (3)
I2	0.43480 (3)	0.20130 (6)	0.37523 (3)
N1	0.3031 (4)	0.1890 (6)	0.1354 (3)
N2	0.2708 (3)	−0.1445 (5)	0.3213 (3)
C1	0.1840 (4)	−0.0550 (7)	0.1486 (3)
C2	0.1643 (4)	0.0035 (7)	0.0584 (3)
C3	0.1028 (4)	−0.0954 (8)	−0.0141 (4)
C4	0.0644 (5)	−0.2492 (8)	0.0066 (5)
C5	0.0865 (4)	−0.3043 (7)	0.0997 (5)
C6	0.1465 (4)	−0.2040 (6)	0.1722 (4)
C7	0.2109 (5)	0.1683 (8)	0.0512 (4)
C8	0.1735 (5)	−0.2352 (7)	0.2748 (4)
C9	0.3861 (5)	0.0896 (11)	0.1176 (5)
C10	0.3312 (6)	0.3726 (8)	0.1473 (5)
C11	0.3560 (6)	−0.2545 (8)	0.3168 (7)
C12	0.2818 (5)	−0.1231 (8)	0.4226 (4)
H31	0.0847	−0.0540	−0.0860
H41	0.0166	−0.3260	−0.0498
H51	0.0570	−0.4238	0.1150
H71	0.2316	0.1718	−0.0120
H72	0.1581	0.2695	0.0494
H81	0.1150	−0.1855	0.3001
H82	0.1824	−0.3697	0.2893
H91	0.4568	0.0955	0.1745
H92	0.3782	0.1278	0.0531
H93	0.3574	−0.0389	0.1106
H101	0.2852	0.4504	0.1767
H102	0.3278	0.4218	0.0794
H103	0.4086	0.3747	0.1934
H111	0.3343	−0.3155	0.2490
H112	0.3491	−0.3439	0.3689
H113	0.4336	−0.2117	0.3352
H121	0.2202	−0.0485	0.4307
H122	0.3528	−0.0701	0.4657
H123	0.2753	−0.2525	0.4440

comparison of observed and calculated structure factor amplitudes (×10, Table III) have been deposited as supplementary material.

Results

Synthesis of [Ni(*NCN'*)X_2] Species. Treatment of the Ni(II) halo complexes [Ni(*NCN'*)X] (**2a–c**) with appropriate oxidizing reagents ($CuCl_2$, $CuBr_2$, and I_2, respectively) readily affords the novel strongly colored complexes [Ni(*NCN'*)X_2] (**1a–c**) in high yield (see Experimental Section). These, the first reported true organometallic Ni(III) species, have recently been used by us as precursors to two further analogues [Ni(*NCN'*)X_2] (X: NO_3, **1d**; NO_2, **1e**). Complexes **1a–e** (Figure 1) are air-stable solids that dissolve reasonably well in CH_2Cl_2, have limited solubility in toluene, and are, for practical purposes, insoluble in diethyl ether. Well-shaped black lustrous crystals are obtained by slow evaporation of CH_2Cl_2/toluene solutions. When powdered, the solids have varied colorings (X: Cl, brown; Br, green; I, purple; NO_3, brown; NO_2, green), and it is these colors that are apparent when they are dissolved in CH_2Cl_2 or toluene. In these two solvents it is believed that these Ni(III) species, which are individually characterized by their UV/visible electronic spectra, exist as isolated nonionic [Ni(*NCN'*)X_2] molecules.

To ascertain unambiguously the structure of these [Ni(*NCN'*)X_2] species in the solid state, a single-crystal X-ray diffraction study of a representative member **1c** has been undertaken.

Solid-State Molecular Structure of [Ni(*NCN'*)I_2] (1c). A perspective view of a single molecule of **1c** demonstrating the atomic numbering scheme adopted is shown in Figure 2. Relevant bond distances and interbond angles are listed in Table IV.

This structural study shows that **1c** crystallizes as discrete monomeric units that are separated by only normal van der Waals distances; a packing diagram (Figure 3) is deposited as supplementary material. The essential stereochemical description of **1c** is a nickel center having a square-based pyramidal ligand array with an iodine atom I1 in the apical site. The basal atoms are a second iodine atom I2 and C1, N1, and N2 of the anionic terdentate ligand *NCN'*. These structural data confirm that **1c** is a true organonickel(III) complex.

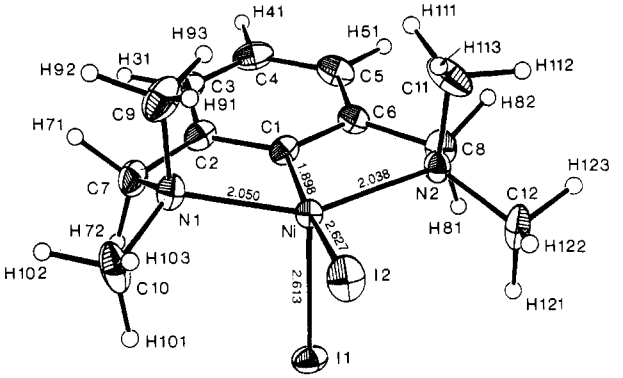

Figure 2. ORTEP plot of [Ni{$C_6H_3(CH_2NMe_2)_2$-*o*,*o*'}I_2] (**1c**) with the adopted numbering scheme.

Table IV. Bond Lengths (Å) and Bond Angles (deg) for [Ni{$C_6H_3(CH_2NMe_2)_2$-*o*,*o*'}I_2] (**1c**)

Ni–I1	2.613 (1)	N2–C12	1.492 (8)
Ni–I2	2.627 (1)	C1–C2	1.376 (7)
Ni–N1	2.050 (4)	C1–C6	1.376 (7)
Ni–N2	2.038 (4)	C2–C3	1.389 (7)
Ni–C1	1.898 (5)	C2–C7	1.471 (8)
N1–C7	1.497 (7)	C3–C4	1.398 (9)
N1–C9	1.492 (8)	C4–C5	1.404 (10)
N1–C10	1.493 (7)	C5–C6	1.388 (7)
N2–C8	1.494 (7)	C6–C8	1.487 (8)
N2–C11	1.491 (8)		
I1–Ni–I2	103.0 (1)	Ni–N2–C11	105.6 (4)
I1–Ni–N1	102.0 (1)	Ni–N2–C12	117.6 (3)
I1–Ni–N2	100.3 (1)	C8–N2–C11	108.7 (5)
I1–Ni–C1	88.2 (2)	C8–N2–C12	108.2 (4)
I2–Ni–N1	95.6 (1)	C11–N2–C1	106.9 (5)
I2–Ni–N2	95.7 (1)	Ni–C1–C2	117.7 (4)
I2–Ni–C1	168.8 (2)	Ni–C1–C6	117.5 (4)
N1–Ni–N2	152.0 (2)	C2–C1–C6	124.6 (5)
N1–Ni–C1	81.9 (2)	C1–C2–C3	117.7 (5)
N2–Ni–C1	82.1 (2)	C1–C2–C7	114.5 (5)
Ni–N1–C7	108.3 (3)	C3–C2–C7	127.8 (5)
Ni–N1–C9	104.5 (4)	C2–C3–C4	119.7 (5)
Ni–N1–C10	117.2 (4)	C3–C4–C5	120.8 (5)
C7–N1–C9	107.3 (5)	C4–C5–C6	119.5 (5)
C7–N1–C10	109.2 (5)	C5–C6–C1	117.7 (5)
C9–N1–C10	109.8 (5)	C5–C6–C8	127.6 (5)
Ni–N2–C8	109.5 (3)	C1–C6–C8	114.7 (4)

The restrictions of the NiC1CCN chelate rings produce significant distortions from an ideal square pyramid (SP) in the direction of a trigonal bipyramid (TBP) with C1 and I2 occupying the axial positions. Use of literature methods[16] to analyze this situation provides a quantitative description of **1c** as a SP with ~20% TBP character.

Details of least-squares planes calculations on **1c** have been deposited as supplementary material (Table V). With respect to the best plane through the basal atoms C1, N1, N2, and I2 (RMSD = 0.109 Å), the nickel atom is displaced 0.325 Å toward I1.

The molecular structure of **1c** has an effective C_s symmetry about the plane through I1, Ni, and C1. The plane of the aryl ring (RMSD = 0.005 Å) is bent out of the basal C1–N1–N2–I2 plane, away from I1, by 11.6°. Both cyclometalated NiC1CCN rings are of essentially skew conformation with their local C_2 axes passing through C1 and bisecting N–C.

The Ni–I bond lengths in **1c** are noticeably different, with the basal bond Ni–I2 being 0.014 Å longer. In the analogous square-pyramidal complex [Fe^{III}(*NCN'*)Cl_2] (not isomorphous

(16) Holmes, R. R. *Prog. Inorg. Chem.* **1985**, *32*, 119–235 and references therein.

Table VI. ESR Data for Ni(III) Complexes **1a–e**

complex	X	g_z	g_y	g_x	A_z[a]	A_y[a]
1a[b]	Cl	2.024	2.195	2.369	28	
1b[b]	Br	2.028	2.190	2.332	140	
1c[b]	I	2.029	2.190	2.326	148	67
1d[c]	NO_3	2.051	2.164	2.322		
1e[c]	NO_2	~2.06	~2.13	2.30		

[a] In gauss. Although both Cl and Br have two isotopes (all $I = {}^3/_2$), hyperfine splitting due to the individual isotopes in **1a** and **1b** was not resolved. [b] Toluene glass. [c] Diglyme glass with added KX; see text.

with **1c**), there is a similar discrimination with the basal Fe–Cl bond being 0.067 Å longer.[17] Because the two halide environments in each of these species are not equivalent, one cannot interpret the different M–X bond distances in terms of the basal M–X bond being the weaker. In fact, EHMO calculations on a model complex $[Ni(C_6H_5)(NH_3)_2I_2]$ with two identical Ni–I bond lengths show that the basal overlap population is greater.[18] Structural studies[18] on closely related [Ni(*NCN'*)I(Y)] (Y = Br, OCHO) show that the Ni–I1 apical bond length in **1c** (2.613 (1) Å) is representative for complexes of this type whereas the Ni–Cl bond length (1.898 (5) Å in **1c**) is more sensitive to the nature of other ligands.

Since **1c** has a square-pyramidal geometry like that of both [Ni(*NCN'*)I(Y)] (Y = Br, OCHO) and $[Fe^{III}(NCN')Cl_2]$,[17] it is worth commenting on the observed stereochemistry of the cyclometalated rings and on how the orientation of the Me groups might affect the metal–ligand sphere. In **1c** the pair of methyl functions H_3C9 and H_3C11 stand axially to their cyclometalated rings and are directed away from the apical iodide ligand, thus appearing to block the coordination site trans to it. At the same time, the equatorial methyl groups H_3C10 and H_3C12 lie in soft van der Waals contact with I2 (I2···C10 = 3.968 Å, I2···C12 = 3.897 Å). The attainment of an octahedral metal coordination geometry requires inversion of a NiC1CCN ring such that the nitrogen atoms come to lie mutually trans and are on opposite sides of the aryl ring plane. Such a process would also transform the corresponding equatorial methyl group into an axial one and position it unfavorably close to the cis iodide ligand I1. However, hexacoordinate Ni(III) species of *NCN'* are feasible; we recently reported the isolation of octahedral $[Ni(NCN')(NCS)_2(C_5H_5N)]$ with trans-coordinated, nonbulky NCS ligands.[8]

Paramagnetism and ESR Spectra of 1a–e. The paramagnetism of [Ni(*NCN'*)X_2] (**1a–e**) was first indicated by our failure to detect ^1H NMR signals from this group of complexes. From the NMR method of Evans,[19] a solution of [Ni(*NCN'*)Br_2] in CH_2Cl_2 gave an approximate value of one unpaired electron per molecule at ~35 °C. An accurate quantification of the paramagnetism of [Ni(*NCN'*)I_2] (**1c**) has been carried out (Faraday method) over the range 80–295 K and has yielded a value of 1.989 (3) μ_B, which confirmed the presence of one unpaired electron. This result indicates a low-spin Ni(III) center, which for a square-pyramidal geometry (vide supra) has the electronic configuration $(d_{xz},d_{yz})^4(d_{xy})^2(d_{z^2})^1(d_{x^2-y^2})^0$.

Further informative data concerning the electronic structure of **1a–e** comes from their ESR spectra, and these data are collected in Table VI. At ambient temperature in toluene all five complexes produce an extremely broad isotropic X-band absorption signal that lacks clear hyperfine structure. The spectra of these solutions of **1a–e** change dramatically on cooling, and when a toluene glass is achieved at ~150 K, the spectral sharpness and fine-structure content are at an optimum. At this temperature each of these dihalo species produces an orthorhombic signal with three distinct g values (see Figure 4). For **1a** (X = Cl) only the g_z shows hyperfine splitting, and its four-line pattern is consistent with coupling to a single chlorine atom. The dibromo and diiodo species **1b** and **1c** provide spectra of a similar type, but the strong overlap of the g_z multiplet with the other signals frustrates straightforward analysis. (To aid analysis, Q-band spectra of **1a–c** were obtained, and under these conditions the g's are separated, though somewhat broadened, and their positions more readily determined.)

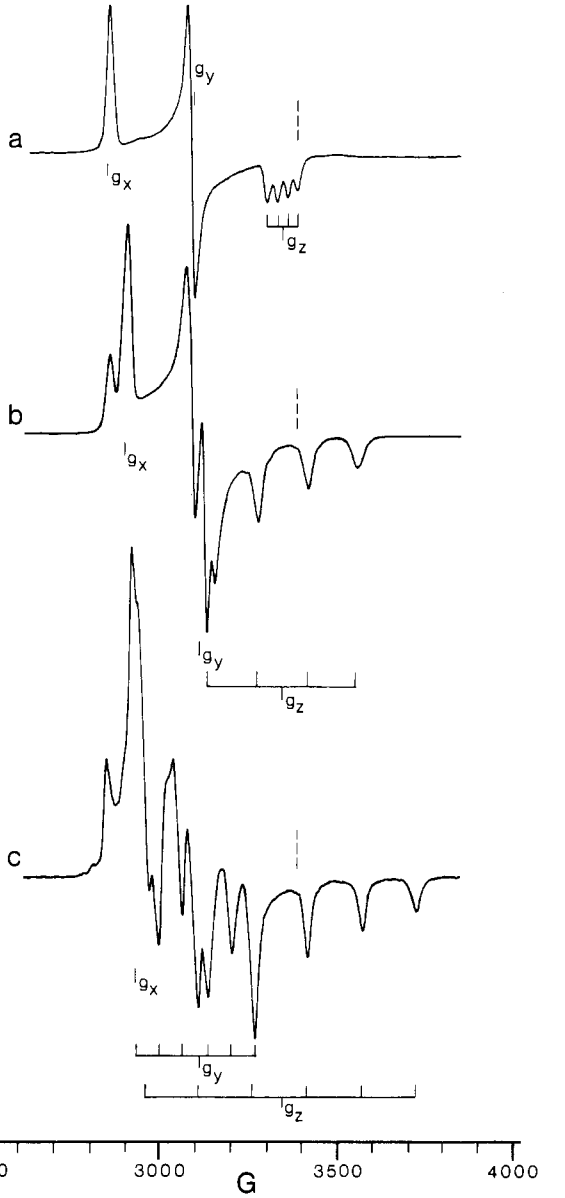

Figure 4. 9.50-GHz X-band spectra of $[Ni^{III}(NCN')X_2]$ species in toluene glasses at ~150 K with $g = 2.002$ indicated by the dashed segment: (a) **1a** (X = Cl); (b) **1b** (X = Br); (c) **1c** (X = I).

Although a few lines in these X-band spectra cannot be explained by using a simple scheme for g splitting, these extra peaks can be satisfactorily reproduced by using computer-based simulations,[20] with good fits to the observed spectra being obtained with the data of Table VI.

The dinitrato and dinitrito species only provided reasonably good ESR data in diglyme glasses at ~160 K (**1d**) and ~135 K (**1e**) in the presence of added KX (see Table VI). The spectrum of **1d** is simple, consisting of three broad g components, none of which exhibit hyperfine splitting. In the case of $[Ni(NCN')(NO_2)_2]$ (**1e**), again three g components can be identified, but these are very broad; further small peaks and shoulders complicate the spectrum, which has not yet been satisfactorily analyzed. These two spectra are shown in Figure 5 (supplementary material).

(17) De Koster, A.; Kanters, J. A.; Spek, A. L.; Van der Zeijden, A. A. H.; Van Koten, G.; Vrieze, K. *Acta Crystallogr. Sect. C: Cryst. Struct. Commun.* **1985**, *C41*, 893–895.
(18) Welch, A. J.; et al., manuscripts in preparation.
(19) Evans, D. F. *J. Chem. Soc.* **1959**, 2003–2005.
(20) POWDER, version 5, 1982 (an ESR simulation program for polycrystalline or glassy materials with Simpson orientation integration).

Table VII. Equivalent Conductivities of Some Nickel Complexes

complex	Λ_0, cm^2 Ω^{-1} equiv^{-1}	
	H_2O	acetone
[Ni(*NCN'*)Cl] (**2a**)	71	
[Ni(*NCN'*)Br] (**2b**)	82	1.5
[Ni(*NCN'*)NO_3] (**2d**)	88	
[Ni(*NCN'*)Br_2] (**1b**)	208	0.5
[Ni(*NCN'*)$(NO_3)_2$] (**1d**)	206	9.9

For **1a–e** the most obvious common feature of their ESR spectra is the orthorhombic signal with three distinct g values for which $\langle g \rangle$ is greater than 2.15. The data of Table VI are fully consistent with these species being examples of low-spin d^7 Ni(III) of low symmetry in which the unpaired electron is primarily based on the nickel atom rather than on any organic moiety. From the magnitude and multiplicity of the hyperfine splittings found in the spectra of **1a–c** it can be concluded, moreover, that this single electron is mostly involved with the unique M–X apical bond, i.e. with the nickel d_{z^2} orbital. In particular, g_z shows coupling to a single halo atom, this being the only resolved splitting in the spectra of **1a** and **1b**. (In **1c**, however, where A_z(I) is only marginally greater than A_z(Br) in **1b**, g_y also exhibits significant coupling to an iodine atom, and an explanation for this is given below.) The spectral line widths of ca. 20–40 G clearly reflect the presence of significant unresolved couplings, but the ^{14}N hyperfine splittings anticipated from the interaction of the nitrogen-donor atoms of *NCN'* with an electron in the d_{z^2} orbital were never actually observed. From the results of EHMO calculations using the analogous model complex [Ni(C_6H_5)$(NH_3)_2I_2$], the same conclusion regarding the position of the unpaired electron is reached and the SOMO (singly occupied molecular orbital) is indicated as being σ-antibonding between nickel and the apical iodide.[18]

The form of the terdentate *NCN'* ligand and the restrictions imposed by the chelate rings in **1a–e** mean that these complexes have intrinsically low symmetry as exemplified by the irregular SP geometry of **1c** (vide supra). As a result the electronic ground state will not be pure d_{z^2} but will contain an admixture of $d_{x^2-y^2}$. This is reflected in the ESR spectra where g_z deviates significantly from the predicted value of 2.00.[21] The result of this mixing on the hyperfine coupling(s) is most evident in the case of **1c** (X = I) where both g_z and g_y show coupling to a single iodine atom. The case for significant mixing of d_{z^2} and $d_{x^2-y^2}$ gains further support from the SOMO calculations of model compound [Ni(C_6H_5)$(NH_3)_2I_2$] using the geometry of **1c**.[18] It is likely that iodo complex **1c** has more pronounced distortions toward a TBP than the chloro or the bromo analogues **1a** and **1b**, consistent with the electronic differences between these halides.

Conductivity and Aqueous Chemistry. The conductivities of acetone and aqueous solutions of [Ni(*NCN'*)X] (X = Br, Cl, NO_3) and [Ni(*NCN'*)X_2] (X = Br, NO_3) were measured in the concentration range (0.4–4) × 10^{-3} mol dm^{-3}, and equivalent conductivities are given in Table VII.[22] In water both the Ni(II) and Ni(III) species are chiefly, if not completely, dissociated as 1:1 and 1:2 electrolytes, respectively. Completion of the nickel coordination sphere would be achieved with water molecules, and the following equilibria are important:

$$\text{Ni(II):}\quad [\text{Ni}(NCN')\text{X}] \overset{H_2O}{\rightleftharpoons} [\text{Ni}(NCN')(H_2O)]^+ + \text{X}^- \quad (1)$$

Ni(III):

$$[\text{Ni}(NCN')\text{X}_2] \overset{H_2O}{\rightleftharpoons} [\text{Ni}(NCN')\text{X}(H_2O)_x]^+ + \text{X}^- \overset{H_2O}{\rightleftharpoons} [\text{Ni}(NCN')(H_2O)_n]^{2+} + 2\text{X}^- \quad (2)$$

In contrast, in acetone (and by inference in other solvents of low dielectric constant) neither **2b** nor **1b** is dissociated. The slight conductivity of [Ni(*NCN'*)$(NO_3)_2$] (**1d**) in acetone could either result from slight dissociation to [Ni(*NCN'*)NO_3]$^+$ (with bidentate-bonded nitrate ion) and NO_3^- or, since **1d** is hygroscopic, result from traces of moisture (vide infra).

These quantitative results are in accord with observations made during synthetic procedures. In particular, **1d** is very soluble in H_2O, affording a pink-brown solution similar in color to that of dilute aqueous solutions of **1a–c**. From the latter, without apparent color change, AgX can be precipitated by addition of Ag^+ ion (as $AgBF_4$). Although this evidence for [$Ni^{III}(NCN')(H_2O)_n]^{2+}$ is very strong, this cation does not appear to have long-term chemical stability in either solution or the solid state, and we have been unable to isolate an analytically pure sample. This contrasts with the Ni(II) situation where solid yellow, somewhat air-sensitive [Ni(*NCN'*)(H_2O)]BF_4 has been isolated and characterized.[4]

Redox Behavior. The ease with which the Ni(II) center of [Ni(*NCN'*)X] may be oxidized is an important aspect of its chemistry, and the redox behavior of both [Ni(*NCN'*)X] and [Ni(*NCN'*)X_2] has been quantified by using normal-pulse and differential-pulse voltammetry and cyclic voltammetry at a platinum electrode in aqueous and acetone solutions. Results are summarized in Tables VIII and IX.

(a) Aqueous Solution. The same half-wave potential, $E_{1/2}$ = +0.14 V (vs SCE), is obtained for the oxidation of [Ni(*NCN'*)X] and the reduction of [Ni(*NCN'*)X_2] independent of X; essentially the same result was also obtained with normal-pulse voltammetry. (The value of 0.21 V for **2d** is probably a result of nitrate absorption at the platinum electrode.) Furthermore, $E_{1/2}$ is also independent of the supporting electrolyte (Bu_4NX; N = Cl, Br, NO_3, PF_6, BF_4) even when X is identical with that originally coordinated to nickel and present in the normal high concentration (0.1 M). In all cases it is clear that the same species are reacting at the electrode, and these must be the hydrated complex ions [$Ni^{II}(NCN')(H_2O)]^+$ and [$Ni^{III}(NCN')(H_2O)_n]^{2+}$, whose existence was also concluded from conductivity measurements (vide supra). Both the width at half-height in differential-pulse cyclic voltammetry ($w_{1/2}$ = 100–125 mV) and the anodic–cathodic peak potential separation in cyclic voltammetry (100–150 mV) are larger than theoretically expected for a one-electron-transfer process (92 and 58 mV, respectively), while the ratio of forward to backward peak heights is close to unity for all complexes. In summary, the Ni(II) and Ni(III) complexes together constitute a quasi-reversible redox couple (eq 3).

$$[\text{Ni}^{II}(NCN')(H_2O)]^+ \underset{+e^-}{\overset{-e^-}{\rightleftharpoons}} [\text{Ni}^{III}(NCN')(H_2O)_n]^{2+} \quad (3)$$

$$E_{1/2} = +0.14 \text{ V (vs SCE)}$$

(b) Acetone Solutions. In this solvent, where complex dissociation is minimal, the ease of oxidation of [Ni(*NCN'*)X] and reduction of [Ni(*NCN'*)X_2] (X = Cl, Br, NO_3) depends strongly upon X, as expressed by the measured peak potentials in the cyclic voltammograms (Table IX). With the appropriate anion present in the solution as supporting electrolyte, the cyclic voltammograms display no essential differences between oxidation of the Ni(II) and reduction of the Ni(III) complexes (see Figure 6). These results are collected in Table IX. The voltammograms show, starting at 0.0 V, that the Ni(III) complex is formed concurrently with the electrochemical oxidation of [Ni(*NCN'*)X] and, furthermore, that the latter Ni(II) species is formed immediately during reduction of [Ni(*NCN'*)X_2]. With increasing scan rates, the waves become more and more drawn out;[23] the charge-transfer processes are thus slow (probably rate determining), and the reaction of X^- with the redox products is presumably faster than the electron-transfer process itself. Because of the different structures of the Ni(II) and Ni(III) complexes, it is to be stressed

(21) Maki, A. H.; Edelstein, N.; Davidson, A.; Holm, R. H. *J. Am. Chem. Soc.* **1964**, *86*, 4580–4590.

(22) Plots of Λ vs $c^{1/2}$ are linear in this range and were extrapolated to zero concentration to afford Λ_0. Water and acetone both give Λ_0 values of 100–150 cm^2 Ω^{-1} mol^{-1} for 1:1 electrolytes: Geary, G. *Coord. Chem. Rev.* **1971**, *7*, 81.

(23) No other change, other than the expected shift in peak potentials, is observed (see: Bard, A. J.; Faulkner, L. R. *Electrochemical Methods Fundamentals and Applications*; Wiley: New York, 1980; p 223), and the existence of intermediates such as [$Ni^{III}(NCN')X]^+$ and [$Ni^{II}(NCN')X_2]^-$ is not indicated.

Table VIII. Electrochemical Data for [Ni(*NCN*')X$_2$] and [Ni(*NCN*')X] Complexes in Water[a]

compd	supporting electrolyte	differential-pulse polarography		cyclic voltammetry[b]			
		E_p, V	$w_{1/2}$,[c] mV	$E_{p,a}$, V	$E_{p,c}$, V	$E_{1/2}$,[d] V	i_b/i_f
		Reductions					
[Ni(*NCN*')Cl$_2$] (**1a**)	Bu_4NCl	0.14	114	0.19	0.09	0.14	0.97
[Ni(*NCN*')Br$_2$] (**1b**)	Bu_4NBr	0.14	105	0.18	0.10	0.14	0.99
	KPF_6	0.15	102	0.21	0.08	0.14	0.95
	$NaBF_4$	0.13	116	0.19	0.04	0.11	0.97
[Ni(*NCN*')(NO$_3$)$_2$] (**1a**)	Bu_4NNO_3	0.14	126	0.21	0.06	0.13	0.91
	$NaBF_4$	0.14	115	0.20	0.09	0.14	0.94
		Oxidations					
[Ni(*NCN*')Cl] (**2a**)	Bu_4NCl	0.13	113	0.17	0.09	0.13	0.88
[Ni(*NCN*')Br] **2b**	Bu_4NBr	0.15	105	0.19	0.11	0.15	0.90
	KPF_6	0.14	108	0.20	0.08	0.14	0.89
	$NaBF_4$	0.14	108	0.22	0.08	0.15	0.81
[Ni(*NCN*')NO$_3$] (**2d**)	Bu_4NNO_3	0.16	133	0.26	0.06	0.16	0.94
	KPF_6	0.14	107	0.20	0.09	0.14	0.93
	$NaBF_4$	0.14	113	0.20	0.09	0.14	0.86

[a] Potentials referred to SCE. [b] Scan rate 200 mV s^{-1}. $E_{p,a}$ and $E_{p,c}$ are the forward peaks for oxidation and reduction, respectively. [c] $w_{1/2}$ is the peak width at half-height. [d] $E_{1/2} = {}^1/_2(E_{p,a} + E_{p,c})$.

Table IX. Electrochemical Data for [Ni(*NCN*')X$_2$] and [Ni(*NCN*')X] Complexes in Acetone[a]

compd	supporting electrolyte X$^-$ (Bu_4NX)	cyclic voltammetry[b]	
		$E_{p,f}$, V	$E_{p,b}$, V
	Reductions		
[Ni(*NCN*')Cl$_2$] (**2a**)	Cl^-	−0.19	0.57
[Ni(*NCN*')Br$_2$] (**2b**)	Br^-	0.05	0.24
	ClO_4^-	0.16	0.39
[Ni(*NCN*')(NO$_3$)$_2$] (**2d**)	NO_3^-	−0.10	0.59
	Cl^-	−0.22	0.73
	Oxidations		
[Ni(*NCN*')Cl] (**1a**)	Cl^-	0.52	−0.17
[Ni(*NCN*')Br] (**1b**)	Br^-	0.24	0.07
[Ni(*NCN*')NO$_3$] (**1d**)	NO_3^-	0.57	−0.07

[a] Peak potentials vs Ag/AgCl (0.1 M LiCl–acetone) reference electrode ($E_{1/2}$ for Fc^+/Fc is +0.63 V) at a scan rate of 200 mV s^{-1}. [b] $E_{p,f}$ is the cathodic peak for the reductions and the anodic peak for the oxidations.

that the anodic and cathodic waves represent two distinct charge-transfer processes (eq 4 and 5) and there is consequently no electrochemical relationship between these two reactions.

$$X^- + [Ni^{II}(NCN')X] \xrightarrow[\text{acetone}]{-e^-} [Ni^{III}(NCN')X_2] \quad (4)$$

$$[Ni^{III}(NCN')X_2] \xrightarrow[\text{acetone}]{+e^-} [Ni^{II}(NCN')X] + X^- \quad (5)$$

The importance of having the appropriate anion present is solution was demonstrated by the oxidation of [Ni(*NCN*')Br] in 0.1 M Bu_4NClO_4; the complex cyclic voltammogram with three irreversible waves at 0.37, 0.70, and 0.85 V and with waves of different current intensity at 0.71 and 0.27 V in the backward scan (scan speed 200 mV s^{-1}) indicates formation of several species. However, with the reduction of [Ni(*NCN*')X$_2$] (X = Br, NO_3) in 0.1 M PF_6^- (or ClO_4^-), a sufficient concentration of X^- builds up around the electrode (eq 5) to allow in the backward scan the reoxidation of the newly formed Ni(II) species (eq 4). Indeed, cyclic voltammograms obtained were similar to those observed for the oxidation of pure **2b** and **2d** with Bu_4NX (X = Br, NO_3), though with higher peak potentials.

Interestingly, the oxidation of [Ni(*NCN*')NO$_3$] in 0.1 M PF_6^- produces a cyclic voltammogram indicative of a quasi-reversible redox couple; peak potentials $E_{p,f}$ = 0.75 V and $E_{p,b}$ = 0.60 V (i_b/i_f = 0.78) at 200 mV s^{-1} scan rate are shifted to values of 0.84 and 0.45 V, respectively, at 10 V s^{-1}. Our interpretation of this result is that a redox couple exists ($E_{1/2}$ = +0.69 V vs Ag/AgCl; differential-pulse polarography (DPP)) in which nitrate functions

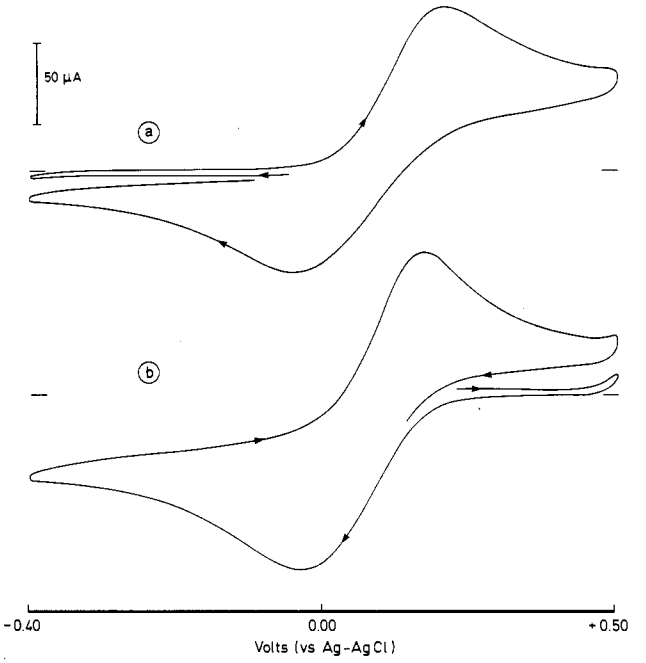

Figure 6. Cyclic voltammetric scans of 10^{-3} M complex solutions at a platinum electrode in acetone (0.1 M Bu_4NBr; scan rate 0.20 V s^{-1}): (a) oxidation of [Ni^{II}(*NCN*')Br] (**2b**); (b) reduction of [Ni^{III}(*NCN*')Br$_2$] (**1b**).

alternatively as a mono- and a bidentate ligand, depending on the oxidation state of the nickel ion[24] (eq 6).

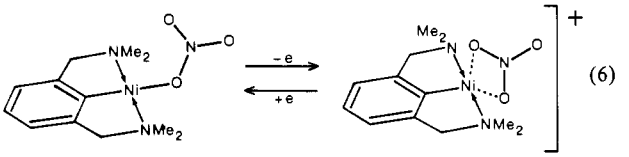

(6)

$E_{1/2}$ = +0.69 V vs Ag/AgCl (from DPP)

Discussion

Although the organic chemistry of nickel is well developed,[25] there is comparatively little known about organo species of Ni(I) and Ni(III) that are believed to play a very important role in many reactions. The study of the uncommon oxidation states of nickel

(24) Jolly, P. W.; Wilke, G. *The Organic Chemistry of Nickel*; Academic: New York, 1974, 1975; Vols. 1, 2.
(25) Kochi, J. K. *Organometallic Mechanisms and Catalysis*; Academic: New York, 1978.

has continuing importance, and its significance has been emphasized by recent reports of paramagnetic nickel centers in certain hydrogenases.[2] The organonickel complexes [Ni(*NCN'*)X_2] (**1a–e**) described in this paper provide a new perspective on the chemistry of the Ni(III) state.

Synthesis and Mechanism. The presence of a kinetically stable nickel–C_{aryl} bond in these new organometallic complexes is excellent supporting evidence for the postulate that species with Ni^{III}–C σ-bonds are intermediates in the oxidative addition of aryl or alkyl halides to Ni(0) substrates.[26] Interestingly, the reaction of *NCN'*Br with [Ni(COD)$_2$], which is a reaction of this type affording principally [Ni(*NCN'*)Br], does yield small amounts of [Ni(*NCN'*)Br_2]. This reaction is thus likely to have a radical mechanism in which the pathway (7) dominates. Side reactions

$$\text{Ni(0)} + \textit{NCN'}\text{Br} \rightarrow [\text{Ni(I)}^+ + \textit{NCN'}\text{Br}^{\bullet -}] \rightarrow [\underset{\mathbf{2b}}{\text{Ni}^{II}(\textit{NCN'})\text{Br}}] \quad (7)$$

8–10, leading to both Ni(II) and Ni(III) products, can be envisaged.

$$\textit{NCN'}\text{Br}^{\bullet -} + \text{Ni(0)} \rightarrow [\text{Ni}^{I}(\textit{NCN'})] + \text{Br}^- \quad (8)$$

$$[\text{Ni}^{I}(\textit{NCN'})] + \textit{NCN'}\text{Br} \rightarrow [\underset{\mathbf{2b}}{\text{Ni}^{II}(\textit{NCN'})\text{Br}}] + {}^1/_2(\textit{NCN'})_2 \quad (9)$$

$$\text{Ni(I)}^+ + \textit{NCN'}\text{Br} \rightarrow [\text{Ni}^{III}(\textit{NCN'})\text{Br}]^+ \xrightarrow{\text{Br}^-} [\underset{\mathbf{1b}}{\text{Ni}^{III}(\textit{NCN'})\text{Br}_2}] \quad (10)$$

Previous studies provide a clear insight into the likely mechanism by which [Ni^{II}(*NCN'*)X] complexes are oxidized by electrophilic reagents such as $Cu^{II}X_2$, $Ag^{I}X$, I_2, and halocarbons to various Ni(III) species. The synthesis of **1c**, for example, from [Ni(*NCN'*)I] and I_2 probably involves initial formation of a donor Ni(II)-to-I_2 complex analogous to the unusual iodine complex [Pt(*NCN'*)I(η^1-I_2)].[27] A one-electron transfer from metal to iodine can occur as shown in eq 11 and 12. The I• radical formed

$$[\text{Ni}^{II}(\textit{NCN'})\text{I}(\eta\text{-I}_2)] + [\text{Ni}^{II}(\textit{NCN'})\text{I}] \rightarrow 2[\text{Ni}^{III}(\textit{NCN'})\text{I}_2] \quad (11)$$

$$[\text{Ni}^{II}(\textit{NCN'})\text{I}(\eta\text{-I}_2)] \rightarrow [\text{Ni}^{III}(\textit{NCN'})\text{I}_2] + \text{I}^\bullet \quad (12)$$

in eq 12 can either recombine as I_2 or interact directly with a Ni(II) substrate to form [Ni^{III}(*NCN'*)I_2] directly.

Similarly, the oxidation reaction of CuX_2 (or AgX) with [Ni(*NCN'*)X] to form the corresponding Ni(III) species is likely to involve an initial interaction of the filled d_{z^2} orbital of the nickel center with the metal salt. A subsequent inner-sphere one-electron ligand-transfer oxidation then affords the Ni(III) product and CuX or Ag(0). In this type of reaction the importance of the two hard donor N atoms of the *NCN'* ligand in determining the nature of the metal center (and hence the d_{z^2} orbital) can be deduced from the fact that closely related [Ni^{II}{$C_6H_3(CH_2PPh_2)_2$-*o,o'*}X] complexes[24] are not similarly oxidized to Ni(III) analogues.

Electrochemistry. Our electrochemical measurements serve to quantify the effect of the *NCN'* ligand on the metal center in both Ni(II) and Ni(III) complexes. What is most notable is the remarkably low value of +0.14 V (vs SCE) for $E_{1/2}$ of the [Ni^{II}(*NCN'*)(H_2O)]$^+$/[Ni^{III}(*NCN'*)(H_2O)$_n$]$^{2+}$ couple. Similarly, the oxidation potentials for the complexes [Ni^{II}(*NCN'*)X] (X = Cl, Br, NO_3) varying between +0.24 and +0.57 V (vs Ag/AgCl, 0.1 M LiCl/acetone) emphasize the ease of the oxidation from Ni(II) to Ni(III) and also show how variation of the X group is a simple and effective way of controlling the properties of the metal center.

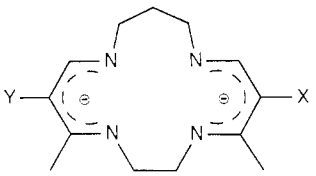

Figure 7. The X,Y-Me_2[15]tetraeno-N_4 ligand system (**I**).

Literature values of $E_{1/2}$ for the Ni(II)/Ni(III) redox couple in coordination complexes cover a wide range reflecting the variety of ligands used.[3] Typical values are in the range +0.5 to +1.5 V (vs SCE), and dianionic N_4 macrocyclic ligand systems such as I are required (Figure 7) to achieve data comparable to those obtained with the *NCN'* ligand.[28] In our system, where Ni(III) complexes of *NCN'* are mild oxidizing agents, reduction through to Ni(I) is expected, empirically, to be difficult.

Structure and ESR. Comparison of the structural parameters of **1c** with those of other Ni(III) species is not particularly fruitful owing to the geometric distortions resulting from the restrictive chelate rings. However, **1c** does provide a value of the Ni(III) covalent radius of ca. 1.3 Å which can be compared to the calculated 1.2 Å in [$NiBr_3(PPhMe_2)_2$][29] and to 1.24 Å obtained from a recent EXAFS study.[2b] Looking more closely at nickel *NCN'* complexes, one sees there are significantly longer Ni–N and Ni–C bonds in **1c** (2.044 (4) Å average and 1.898 (5) Å, respectively) than in [Ni^{II}(*NCN'*)OCHO] (**2f**) (1.9745 (1) Å average and 1.814 (2) Å, respectively); clearly, the effect of geometry change dominates over any tendency of bond lengths to shorten as the formal metal charge increases from +2 to +3. A similar effect appears in octahedral [Ni^{III}(*NCN'*)$(NCS)_2$py], where the corresponding bond lengths are also longer than those in **2f**.[8]

The various metal coordination spheres observed in *NCN'* complexes of Ni(III) are partially determined by the electronic properties of the remaining ligands and the way these affect, in combination with *NCN'*, the ordering of the metal d orbitals. Qualitatively, one sees stabilization of square-pyramidal [Ni(*NCN'*)X_2] by Cl^-, Br^-, and even I^-, the similarity of their structures being reflected in their similar ESR *g* values. With SCN^-, however, [Ni^{III}(*NCN'*)$(NCS)_2$] has, to date, not been isolated owing to a strong tendency for formation of octahedral [Ni^{III}(*NCN'*)$(NCS)_2$(donor molecule)] species.[8] This is in line with the position of SCN^- in the spectrochemical series. Likewise, the position of NO_3^- and NO_2^- in this series suggests that they also should not be particularly suitable for stabilizing pure five-coordinate Ni(III) when monodentate bonded, and the available evidence supports this. First, both **1d** and **1e** dissociate in H_2O far more readily than **1a–c** to produce [Ni^{III}(*NCN'*)(H_2O)$_n$]$^{2+}$; this type of dissociation of complexes of general type [$Ni^{III}LX_2$]$^{n+}$ is well documented.[30] Second, although **1d** and **1e** are isolable, their ESR data point to structures somewhat different from those of **1a–c**, and in these cases it is possible that the NO_3^- and NO_2^- ions are using the potential of their multidentate nature to stabilize the Ni(III) centers with pseudooctahedral geometries. The solution electrochemistry study of [Ni(*NCN'*)NO_3] also produced evidence of bidentate NO_3^- in a Ni(III) species. The three characteristic *g* values observed in the ESR spectra of **1a–e** are a direct result of the asymmetry imposed on the d^7 ion through the combined coordination of chelate *NCN'* and two other anions. Most reported Ni(III) coordination complexes have an approximately square-planar metal center and therefore have a somewhat higher symmetry than **1a–c** and generally exhibit axially symmetric spectra where $g_\perp > g_\parallel$. Three components are however sometimes identifiable in peptide complexes of Ni(III) ($g_\perp \sim g_\perp' > g_\parallel$) as a result of tetragonal distortions of the octahedral array brought about by varying degrees of donor ligand coordination.[3,31]

(26) Monodentate nitrate bonding has been identified in the related phosphine complex [Pd{$C_6H_3(CH_2PPh_2)_2$-*o,o'*}NO_3]: Rimml, H. Ph.D. Thesis No. 7562, ETH Zürich, 1984.

(27) Like **1c**, this unique complex has a square-pyramidal geometry. It has an η-I_2 in a linear Pt–I–I unit: Van Beek, J. A. M.; van Koten, G.; Smeets, W. J. J.; Spek, A. L. *J. Am. Chem. Soc.* **1986**, *108*, 5010–5011.

(28) Busch, D. H. *Acc. Chem. Res.* **1978**, *11*, 392–400.

(29) Stalik, J. K.; Ibers, J. A. *Inorg. Chem.* **1970**, *9*, 453–458.

(30) (a) Gore, E. S.; Busch, D. H. *Inorg. Chem.* **1973**, *12*, 1–3. (b) Lovecchio, F. V.; Gore, E. S.; Busch, D. H. *J. Am. Chem. Soc.* **1974**, *96*, 3109–3118. (c) Bencini, A.; Fabbrizzi, L.; Poggi, A. *Inorg. Chem.* **1981**, *20*, 2544–2549.

Almost invariably $g_\perp$ and $g_\perp'$ are broadened (variously ascribed to unresolved hyperfine splitting or g strain), and this contrasts with the situation for **1a–c** (but not **1d** and **1e**), where the lines are comparatively sharp.

In other recent studies we have identified further examples of paramagnetic *NCN'* metal complexes, i.e. $[FeCl_2(NCN')]$[17] (SP, high-spin) and $[CoX(NCN')L]$[32] (SP, low-spin). The Co(II) species, which have ESR data comparable to those of **1a–c**, were principally identified on the basis of spectroscopic (ESR, UV) measurements, and the relevant d-orbital ordering in Ni(III) and Co(II) d^7 species of *NCN'* has been fully described.[32]

Nickel Hydrogenases. It is now well established that certain hydrogenases contain a nickel center that in its oxidized form is a low-spin Ni(III) d^7 ion that gives rise to rhombic ESR spectra. There is evidence that one or more sulfur atoms are in the ligand sphere, and there is continuing research into the identification of the other ligating atoms and the metal geometry. Significantly, the g values of **1a–c** not only are similar to those obtained from the hydrogenases but also, unlike the situation with the Ni(III) peptide complexes, have comparably narrow line widths. This information together with the firmly established structure of **1c** makes these novel organometallic species an important reference point when one postulates and tests possible structures for the enzyme centers. In particular, **1a–c** show that it is possible with the appropriate geometry to have N donors present without necessarily producing broad ESR signals. Secondly, they show that a nickel center with a square-pyramidal array, i.e. with a vacant coordination site, could be the active center in the hydrogenase enzymes. Finally, since the value of the Ni^{2+}/Ni^{3+} redox couple of = +0.14 V vs SCE for the aquated $[Ni(NCN')]$ system is low compared to most other inorganic systems (including the peptide complexes), it can be inferred that oxygen (and hence sulfur) donors must be important in the hydrogenases,[33] where the value of this couple is typically −0.2 V (vs SHE).

Conclusions

The Ni(III) state, an electronic configuration which had hitherto been associated primarily with inorganic and coordination complexes, has now been shown to be a stable and readily accessible oxidation state in true organonickel species. The structural characterization of five-coordinate $[Ni(NCN')I_2]$, confirming a direct Ni–C bond, when combined with spectroscopic, conductivity, and electrochemical evidence adds a new dimension to the discussions regarding the nature, stability, and occurrence of tervalent nickel in organic and bioinorganic systems.

Acknowledgment. Dr. S. P. J. Albracht is thanked for many helpful discussions and for the measurement of Q-band ESR spectra.

Registry No. **1a**, 84500-90-3; **1b**, 84520-52-5; **1c**, 84500-91-4; **1d**, 84500-92-5; **1e**, 84500-93-6; **2a**, 84500-94-7; **2b**, 99532-40-8; **2c**, 99532-41-9; **2d**, 89618-54-2.

Supplementary Material Available: For **1c**, Tables II and V, listing anisotropic thermal parameters and least-squares planes, and Figure 3, showing a packing diagram of the unit cell, and for **1d** and **1e**, Figure 5, showing 9.50-GHz X-band ESR spectra of $[Ni^{III}(NCN')X_2]$ species in diglyme at ~150 K in the presence of added KX (4 pages); Table III, listing observed and calculated structure factors (20 pages). Ordering information is given on any current masthead page.

(31) (a) Lappin, A. G.; Murray, C. K.; Margerum, D. W. *Inorg. Chem.* **1978**, *17*, 1630–1634. (b) Sugiura, Y.; Mino, Y. *Inorg. Chem.* **1979**, *18*, 1336–1339. (c) Sugiura, Y.; Kuwahara, J.; Suzuki, T. *Biochem. Biophys. Res. Commun.* **1983**, *115*, 878–881.
(32) Van der Zeijden, A. A. H.; Van Koten, G. *Inorg. Chem.* **1986**, *25*, 4723–4725.
(33) Ray, D.; Pal, S.; Chakravorty, A. *Inorg. Chem.* **1986**, *25*, 2674–2876.

Contribution from 3M Corporate Research Laboratories and 3M Commercial Chemicals Division Laboratory, St. Paul, Minnesota 55144

Protonation of Cobalt, Rhodium, and Iridium Hydrides with Fluorocarbon Acids. Synthesis, Reactivity, and Dynamic Properties of $(Ph_3P)_3Rh^+$ and Its Derivatives

A. R. Siedle,*[†] R. A. Newmark,[†] and R. D. Howells[‡]

Received December 8, 1987

Protonation of a variety of Co, Rh, and Ir hydrides with the fluorocarbon acids $H_2C(SO_2CF_3)_2$, $PhCH(SO_2CF_3)_2$, $HN(SO_2CF_3)_2$, $H_2C(SO_2C_8F_{17})_2$, and $C_8F_{17}SO_3H$ is reported. The Co and Ir hydrides form cationic dihydrides. Protonation of $(Ph_3P)_4RhH$ affords $[(Ph_3P)_3Rh][HC(SO_2CF_3)_2]$. The stereochemical nonrigidity of $[(Ph_3P)_3Rh]^+$ in solution has been characterized by ^{31}P DNMR. Reactions of this 14-electron Rh(I) compound are described, including the solid-state carbonylation to yield $[(Ph_3P)_3Rh(CO)_2][HC(SO_2CF_3)_2]$. Carbon monoxide in the dicarbonyl salt is labile, and it dissociates in solution to give $[(Ph_3P)_3Rh(CO)][HC(SO_2CF_3)_2]$. Fluorocarbon acids having long-chain perfluoroalkyl groups are useful in synthesizing salts that have high solubility in aromatic hydrocarbons.

Introduction

Reactions of protons with transition-metal hydrides are of considerable fundamental importance in organometallic and catalytic chemistry. Idealized protonation of such hydrides, M–H, represented by eq 1, can occur in ion cyclotron resonance ex-

$$M\text{–}H + H^+ \rightarrow MH_2^+ \rightarrow M^+ + H_2 \qquad (1)$$

periments[1] but are infrequently observed in fluid solution[2] because MH_2^+ and coordinatively unsaturated M^+ species tend to interact strongly with both counterions and nucleophilic solvents. Our approach to the study of inorganic proton-transfer reactions involves the use of bis((perfluoroalkyl)sulfonyl)alkanes in hydrocarbon solvents.[3–8] These fluorocarbon acids, of which $H_2C(SO_2CF_3)_2$ (**1**) and $PhCH(SO_2CF_3)_2$ (**2**) are exemplary, possess an unusual constellation of properties. They are strong, carbon-centered protic acids that are nonoxidizing, nonhygroscopic, and soluble in noncoordinating solvents such as toluene and di-

[†] 3M Corporate Research Laboratories.
[‡] 3M Commercial Chemicals Division Laboratory.

(1) Beauchamp, J. L.; Stevens, A. E.; Corderman, R. R. *Pure Appl. Chem.* **1979**, *51*, 967.
(2) Muetterties, E. L.; Watson, P. L. *J. Am. Chem. Soc.* **1978**, *100*, 6978.
(3) An alternate strategy utilizes neat CF_3SO_3H as both proton source and solvent. In this way, coordinatively unsaturated $Mn(CO)_5^+$ has been obtained: Trogler, W. C. *J. Am. Chem. Soc.* **1979**, *101*, 6459.
(4) Siedle, A. R.; Newmark, R. A.; Pignolet, L. H.; Howells, R. D. *J. Am. Chem. Soc.* **1984**, *106*, 1510.
(5) Siedle, A. R.; Newmark, R. A.; Pignolet, L. H. *Organometallics* **1984**, *3*, 855.
(6) Siedle, A. R.; Newmark, R. A.; Pignolet, L. H.; Wang, D. X.; Albright, T. A. *Organometallics* **1986**, *5*, 38.
(7) Siedle, A. R.; Newmark, R. A.; Pignolet, L. H. *Inorg. Chem.* **1986**, *24*, 1345.
(8) Siedle, A. R.; Newmark, R. A.; Pignolet, L. H. *Inorg. Chem.* **1986**, *25*, 3412.

0020-1669/88/1327-2473$01.50/0